Hierarchical Nanostructures of Organosilicate Nanosheets within Self-Organized Block Copolymer Films

**Tomoyasu Hirai,[†,‡] Melvina Leolukman,[†]
Teruaki Hayakawa,*[,‡] Masa-aki Kakimoto,[‡] and
Padma Gopalan*[,†]**

*Department of Materials Science and Engineering,
University of Wisconsin—Madison, Madison, Wisconsin
53706, and Department of Organic and Polymeric Materials,
Tokyo Institute of Technology, 2-12-1-S8-26 O-okayama,
Meguro-ku Tokyo 152-8552, Japan*

*Received April 19, 2008
Revised Manuscript Received May 20, 2008*

The thermodynamically driven process of spontaneous self-assembly of block copolymers (BCP's)[1] has inspired a range of functional materials where domain confinement is of importance. The self-assembled structures can range in sizes from a few hundred nanometers to sub-30 nm, depending on the architecture, chemical composition, and degree of polymerization.[2] The shorter length scales are particularly interesting for tuning the electronic and optical properties of molecules and creating templates for nanopatterning,[3] whereas the submicron length scales are potentially useful for photonic band gap materials.[4] Recently, a variety of hierarchical structures, primarily defined as smaller length scale ordered crystalline or liquid crystalline domains within a larger microphase-separated structure arising from self-assembly of organic−organic BCP's, have been reported.[5] On the other hand, very few attempts have been made to study the formation of well-defined organic−inorganic hierarchical structures. Organic−inorganic hybrid BCP's are of interest to enhance the thermal, dielectric, and mechanical properties. These hybrid materials with multiple length scales of ordering are of great interest for nanopatterning where in a single step a soft mask can be converted into a hard mask.[6]

The precursors for creating the inorganic block predominantly contain either silicon or iron.[7] One such example of an inorganic precursor is polyhedral oligomeric silsesquioxane (POSS), which has been used extensively to create polymer composites. POSS segments in a polymer are known to form nanometer size crystalline or glassy aggregates[8] which are converted to silica on exposure to oxygen plasma.[9] There are reports on the synthesis of random copolymers containing POSS units by conventional free radical polymerization,[10] ring-opening metathesis polymerization,[11] and on POSS-terminated block copolymers.[12] In the case of random copolymers containing POSS, lamella-like POSS aggregates were reported, but they lacked long-range order due to the random nature of the copolymer. Whereas, the POSS-terminated block copolymer results in well-ordered lamella structure, but the dimensions of the POSS domains were not tunable. One approach to create a truly hierarchical structure where the POSS cages are ordered into sheets within the microphase-separated domains is to synthesize BCP's from monomers containing a POSS cage, hence allowing tunable sheet length.

Table 1. Molecular Weight and Molecular Weight Distribution of PMMA-*b*-PMAPOSS and PS-*b*-PMAPOSS

sample[a]	M_n[b] (g mol^{-1})	M_n[c] (g mol^{-1})	PDI
PMMA$_{188}$-*b*-PMAPOSS$_{30}$	47 700	28 200	1.08
PS$_{257}$-*b*-PMAPOSS$_{21}$	47 000	20 200	1.05

[a] The number refers to the final composition determined from the gel permeation chromatography (GPC) results and integration from ^{1}H NMR spectra. [b] BCP molecular weight determined by GPC, calibrated against PS linear standards. [c] Molecular weight of PMAPOSS segment determined from the GPC results and integration from ^{1}H NMR spectra.

Several methods have been reported toward the synthesis of the POSS side chain containing BCP's. Pyun et al. have demonstrated the atom transfer radical polymerization (ATRP) of methacrylate-functionalized POSS. In this case, the degree of polymerization (DP) was less than 15 since the steric hindrance of POSS inhibits the forming of copper(I) complex with chain ends.[8b,13] In a previous work, we demonstrated that hydrosilylation of polystyrene-*b*-poly(1,2-*ran*-3,4-isoprene) [PS-*b*-PI] with hydridoheptacyclopentyl-substituted POSS resulted in the incorporation of POSS in the PI domain (PS-*b*-PIPOSS). As expected, the postfunctionalization reaction did not incorporate POSS to all the PI units.[14] In both of these cases while phase separation was observed, no hierarchical structures consisting of the ordered crystalline POSS domains were obtained. We believe that since POSS aggregation is the driving force for ordering of POSS units within the microphase-separated BCP domains for formation of the hierarchical structure, it is important to control both the polydispersity index (PDI) and the length of the POSS chain precisely. Here, we report living anionic polymerization of methacrylate-functionalized POSS, resulting in high DP of the POSS chain and narrow PDI leading to the ordering of the POSS units within the microphase-separated domains.

Two kinds of POSS-containing BCP's, namely PMMA-*b*-PMAPOSS and PS-*b*-PMAPOSS, were synthesized by living anionic polymerization. The synthesis scheme is illustrated in Figure 1. Both reactions were carried out in 10-fold excess of LiCl and 4-fold excess of 1,1-diphenyletylene (DPE) as both methyl methacrylate (MMA) and 3-(3,5,7,9,11,13,15-heptaisobutyl-pentacyclo[9.5.1^{3,9}.1^{5,15}1^{7,13}]octasiloxan-1-yl)propyl methacrylate (MAPOSS) have carbonyl groups. *sec*-BuLi initiator and the living chain of polystyrene (PS) are highly reactive reagents and selectively attack carbonyl groups. DPE end-caps the *sec*-BuLi initiator and the living chain of PS, hence inhibiting the highly reactive reagents from attacking MMA carbonyl groups. The end-capped living chain of DPE does not attack another DPE monomer due to a significant steric load and hence exclusively adds MAPOSS, leading to well-controlled polymerization.[15] The chemical structure and composition of the PMMA-*b*-PMAPOSS and PS-*b*-PMAPOSS were characterized by NMR and IR spectrum (see Supporting Information).

The M_n and PDI of PMMA-*b*-PMAPOSS and PS-*b*-PMAPOSS against linear PS standards were $M_n = 47\,700$ g mol^{-1}, PDI 1.08 and $M_n = 47\,000$ g mol^{-1}, PDI 1.05, respectively. The composition of the block copolymer was estimated from ^{1}H NMR spectra. These results are summarized in Table 1. High DP of POSS chain (DP PMMA-*b*-PMAPOSS = 30 and DP

---

* Corresponding authors: Tel 608-265-4258 (P.G.), +81-3-5734-2429 (T.H.); Fax 608-262-8353 (P.G.), +81-3-5734-2875 (T.H.); e-mail pgopalan@wisc.edu (P.G.), hayakawa.t.ac@m.titech.ac.jp (T.H.).
[†] University of Wisconsin—Madison.
[‡] Tokyo Institute of Technology.

10.1021/ma800872v CCC: $40.75

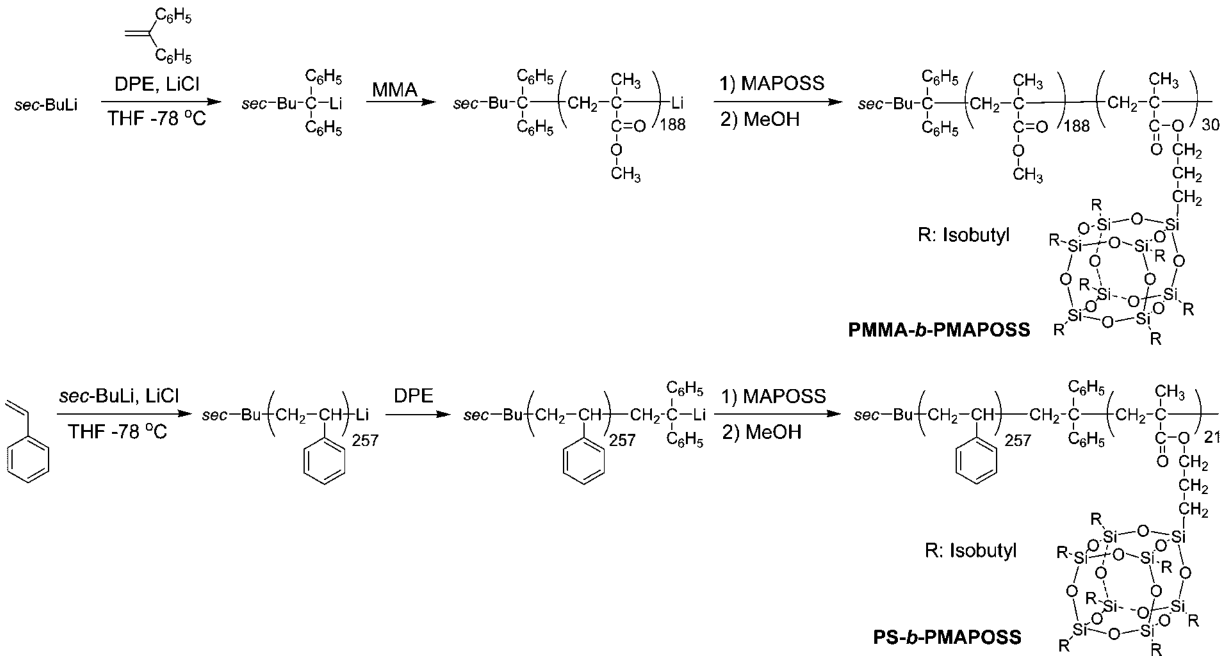

Figure 1. Synthesis of PMMA-*b*-PMAPOSS and PS-*b*-PMAPOSS by living anionic polymerization.

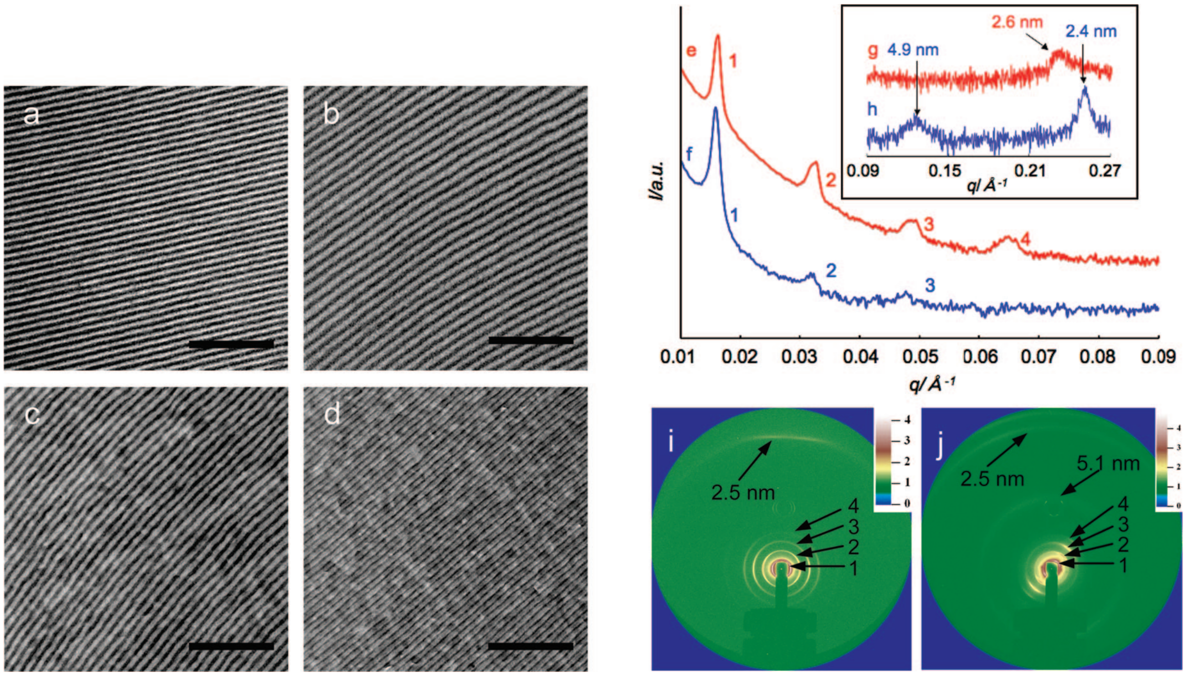

Figure 2. Unstained TEM images from PMMA-*b*-PMAPOSS (a) unannealed and (b) annealed and PS-*b*-PMAPOSS (c) unannealed and (d) annealed (dark regions are PMAPOSS and bright regions are either PS or PMMA; scale bars represent 200 nm). SAXS line profiles of PMMA-*b*-PMAPOSS (e) unannealed and (f) annealed. WAXS line profiles from PMMA-*b*-PMAPOSS (g) unannealed and (h) annealed. WAXS patterns from PS-*b*-PMAPOSS (i) unannealed and (j) annealed.

PS-*b*-PMAPOSS = 21) was successfully obtained by living anionic polymerization.

Bulk morphology of the two POSS-containing block copolymers were examined in samples prepared by slow evaporation from chloroform and then annealed at 190 °C for 24 h. The samples were characterized by transmission electron microscopy (TEM), small-angle X-ray scattering (SAXS), and wide-angle X-ray scattering (WAXS). Figure 2 shows TEM images of unannealed and annealed PMMA-*b*-PMAPOSS and PS-*b*-PMAPOSS. All samples were imaged without staining. The contrast in TEM micrographs is due to the higher mass contrast of silicon-containing POSS compared to PS and PMMA. Well-defined and long-range lamellae structures were obtained for both unannealed and annealed PMMA-*b*-PMAPOSS and PS-*b*-PMAPOSS samples.

Parts e and f of Figure 2 are SAXS line profiles of unannealed and annealed PMMA-*b*-PMAPOSS, respectively. Parts i and j of Figure 2 show WAXS patterns of unannealed and annealed PS-*b*-PMAPOSS, respectively. These results show a peak scattering ratio (q/q^*, where q^* is the position of the primary scattering peak) of 1, 2, and 3, which is consistent with lamellae morphology. In addition to confirming the TEM results, the X-ray results support several interesting observations. First, the *d* spacing in both PMMA-*b*-PMAPOSS (Figure 2e,f) and PS-

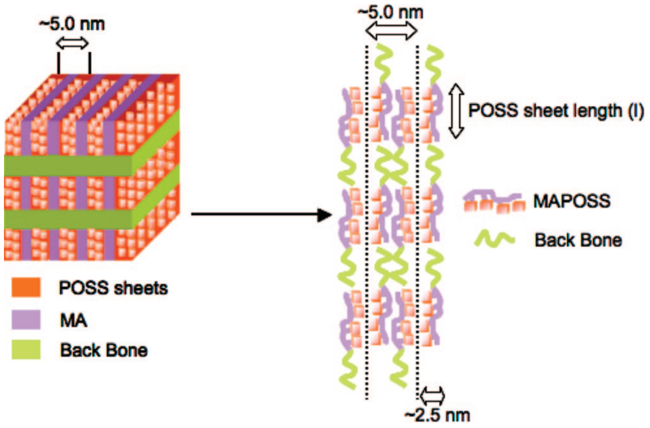

Figure 3. Schematic illustration of hierarchical structure containing POSS sheets in polymer film.

b-PMAPOSS (Figure 2i,j) changes on annealing from 38.7 to 39.7 nm and 37.7 to 40.2 nm, respectively. Second, a new reflection appears at 4.9 nm (PMMA-*b*-PMAPOSS, Figure 2h) and 5.1 nm (PS-*b*-PMAPOSS, Figure 2j) on annealing. Furthermore, for both annealed and unannealed samples a peak was seen close to 2.5 nm.

A schematic representation of the morphology derived from the TEM and X-ray diffraction data is presented in Figure 3. The distance of 2.5 nm is a good agreement with the calculated length between the methacrylate (MA) backbone and POSS cage. After annealing, new reflection appeared at 5 nm, which corresponds to twice the calculated length between the MA backbone and POSS cage. These results indicate a regular array of POSS sheets in the film with a *d* spacing of 5 nm driven by interchain aggregation of POSS units. POSS aggregation will most likely stretch the MAPOSS chain, resulting in the observed increase in *d* spacing. From this model the expected POSS sheet length (*l*) should be the same as PMAPOSS chain length. Therefore, our synthetic methodology for the first time allows control over the POSS sheets length by changing PMAPOSS segment length.

In summary, organic−inorganic BCP's containing POSS namely PMMA-*b*-PMAPOSS and PS-*b*-PMAPOSS were synthesized by living anionic polymerization, with excellent control over the POSS chain length and narrow polydispersity. From TEM and X-ray scattering, well-defined and long-range lamellae structures were obtained for both unannealed and annealed films. Both polymers show a typical reflection at 2.5 nm, which corresponds to the calculated length between MA backbone and POSS cage. The emergence of a new reflection upon annealing at ∼5 nm shows that the POSS units are ordered into sheets with a *d* spacing of 5 nm within the microphase-separated lamellar BCP. The anionic polymerization route we have demonstrated here for synthesizing POSS-containing BCP's overcomes the limitation of other methods such as ATRP, leading to a well-defined hierarchical structure containing POSS sheets in polymer films. These materials containing hierarchical structures can be potentially utilized for creating feature in an ∼10 nm length scale lithographic template.

Acknowledgment. This work was supported by the Semiconductor Research Corporation, the UW-NSF Nanoscale Science and Engineering Center (DMR-0425880), and the Center on Functional Engineered Nano Architectonics (FENA). The authors acknowledge Advanced Photon Source, Argonne National Laboratories, for X-ray diffraction studies.

Supporting Information Available: Experimental procedures, analytical methods, and instrumentation. This material is available free of charge via the Internet at http://pubs.acs.org.

References and Notes

(1) (a) Muthukumar, M.; Ober, C. K.; Thomas, E. L. *Science* **1997**, *277*, 1225. (b) Bates, F. S.; Fredrickson, G. H. *Phys. Today* **1999**, *52*, 32. (c) Bates, F. S. *Science* **1991**, *251*, 898. (d) Bates, F. S.; Fredrickson, G. H. *Annu. Rev. Phys. Chem.* **1990**, *41*, 525.

(2) Urbas, A. M.; Maldovan, M.; Derege, P.; Thomas, E. L. *Adv. Mater.* **2002**, *14*, 1850.

(3) Segalman, R. A. *Mater. Sci. Eng. R* **2005**, *48*, 191.

(4) Park, C.; Yoon, J.; Thomas, E. L. *Polymer* **2003**, *44*, 6725.

(5) (a) Ruokolainen, J.; Mäkinen, R.; Torkkeli, M.; Mäkelä, T.; Serimaa, R.; Brinke, G. T.; Ikkala, O. *Science* **1998**, *280*, 557. (b) Ruokolainen, J.; Brinke, G. T.; Ikkala, O. *Adv. Mater.* **1999**, *11*, 777. (c) Ruokolainen, J.; Saariaho, M.; Ikkala, O. *Macromolecules* **1999**, *32*, 1152. (d) Ikkala, O.; Brinke, G. T. *Chem. Commun.* **2004**, *19*, 2131.

(6) Fukukawa, K.; Zhu, L.; Gopalan, P.; Ueda, M.; Yang, S. *Macromolecules* **2005**, *38*, 263.

(7) (a) Drazkowski, D. B.; Lee, A.; Haddad, T. S.; Cookson, D. J. *Macromolecules* **2006**, *39*, 1854. (b) Rider, D. A.; Cavicchi, K. A.; Power-Billard, K. N.; Russell, T. P.; Manners, I. *Macromolecules* **2005**, *38*, 6931.

(8) (a) Waddon, A. J.; Zheng, L.; Farris, R. J.; Coughlin, E. B. *Nano Lett.* **2002**, *2*, 1149. (b) Pyun, J.; Matyjaszewski, K.; Wu, J.; Kim, G.-M.; Chun, S. B.; Mather, P. T. *Polymer* **2003**, *44*, 2739.

(9) Tegou, E.; Bellas, V.; Gogolides, E.; Argitis, P.; Eon, D.; Cartry, G.; Cardinaud, C. *Chem. Mater.* **2004**, *16*, 2567.

(10) Romo-Uribe, A.; Mather, P. T.; Haddad, T. S.; Lichtenhan, J. D. *J. Polym. Sci., Part B: Polym. Phys.* **1998**, *36*, 1857.

(11) (a) Zheng, L.; Waddon, A. J.; Farris, R. J.; Coughlin, E. B. *Macromolecules* **2002**, *35*, 2375. (b) Zheng, L.; Hong, S.; Cardoen, G.; Burgaz, E.; Gido, S. P.; Coughlin, E. B. *Macromolecules* **2004**, *37*, 8606. (c) Zheng, L.; Farris, R. J.; Coughlin, E. B. *Macromolecules* **2001**, *34*, 8034.

(12) Miao, J.; Cui, L.; Lau, H. P.; Mather, P. T.; Zhu, L. *Macromolecules* **2007**, *40*, 5460.

(13) (a) Pyun, J.; Matyjaszewski, K. *Macromolecules* **2000**, *33*, 217. (b) Pyun, J.; Matyjaszewski, K. *Chem. Mater.* **2001**, *13*, 3436.

(14) Hayakawa, T.; Seino, M.; Goseki, R.; Hirai, T.; Kikuchi, R.; Kakimoto, M.; Tokita, H.; Yokoyama, H.; Horiuchi, S. *Polym. J.* **2006**, *38*, 567.

(15) (a) Kloninger, C.; Rehahn, M. *Macromolecules* **2004**, *37*, 1720. (b) Varshney, S. K.; Hautekeer, J. P.; Fayt, R.; Jérome, R.; Teyssié, Ph. *Chem. Mater.* **1990**, *23*, 2618.

MA800872V